

# Point Spread Function Deconvolution of an Atmospheric Cherenkov Telescope

G.E.Kenny, G.H.Gillanders and M.J.Lang

*Department of Physics, National University of Ireland, Galway, Ireland*

Presenter: G.E. Kenny ([gary.kenny@nuigalway.ie](mailto:gary.kenny@nuigalway.ie)), ire-kenny-GE-abs1-og27-poster

The effect of iteratively deconvolving Imaging Atmospheric Cherenkov Telescope (IACT) images is investigated here with the aim of exploiting the full resolution of an IACT photomultiplier tube camera. The Richardson-Lucy method of de-blurring images was chosen for the study as it functions effectively in the presence of noise. After the Richardson-Lucy algorithm was integrated into the analysis software, the procedure was tested using Crab Nebula data collected with the Whipple 10m IACT. Using the measured Point Spread Function (PSF) of the instrument with the Richardson-Lucy subroutine, Cherenkov images were iteratively deconvolved. Following this, a full re-optimisation of picture and boundary thresholds and image selection parameters was carried out in an attempt to enhance the detected signal. The improvement in signal using this method was not statistically significant.

## 1. Introduction

The results of applying the Richardson - Lucy (R-L) deconvolution algorithm to Cherenkov images in an attempt to enhance the  $\gamma$ -ray signal in Cherenkov data are presented here. The R-L method of deconvolution is an iterative method of restoring degraded or blurred images that has been popular in optical astronomy for many years, and was the favored method of image restoration for early degraded Hubble Space Telescope images [1]. The method considers images, PSFs, and degraded images as probability-frequency functions and then implements Bayes' theorem [2][3]. There are other methods of deconvolution in use in other areas of astronomy. For example, Fourier methods are generally successful at restoring degraded images as long as the noise level in the degraded image is moderate or small [4][5]. The R-L algorithm was chosen for this experiment as it performs well in the presence of elevated noise levels.

## 2. Background

Bayes' Theorem is a simple mathematical formula used for calculating conditional probabilities and in its simplest form can be defined as

$$P(B|A) = \frac{P(A \cap B)}{P(A)}, \quad (1)$$

where  $P(B|A)$  is the probability of observing the event  $B$  given the fact that  $A$  has occurred,  $P(A \cap B)$  is the probability that both  $A$  and  $B$  occur, and  $P(A)$  is the probability of  $A$  in the first place. For our purposes we assume that a blurred image  $H$  can be described by  $H=W*S$ , where  $S$  is the PSF of the instrument,  $W$  is the original image, and  $*$  signifies the mathematical procedure of convolution. Our task here is to extract the original image  $W$  using what we know of the blurred image and the PSF. Here we define Bayes' theorem as

the conditional probability of an event at  $W_i$  given an event at  $H_k$ ,

$$P(W_i|H_k) = \frac{P(H_k|W_i)P(W_i)}{\sum_j P(H_k|W_j)P(W_j)}; \quad (2)$$

$$i = \{1, I\}, \quad j = \{1, J\}, \quad k = \{1, K\}.$$

Here  $H_k$  is an arbitrary cell of  $H$ . Note that in the right side of this equation,  $P(W_i)$  is the desired solution. Since we do not know  $P(W_i)$  when starting the deconvolution process, a common practice [6][7] is to use an estimate for  $P(W_i)$  derived from (2). Following the method described by Richardson [2], we derive

$$W_{i,j,r+1} = W_{i,j,r} \sum_{m=i}^e \sum_{n=j}^f \frac{H_{m,n} S_{m-i+1, n-j+1}}{\sum_{p=a}^b \sum_{q=c}^d W_{q,p,r} S_{m-p+1, n-q+1}}, \quad 1 \quad (3)$$

from (2) for a two dimensional deconvolution iterative process that can then be applied to Whipple 10m Cherenkov data. This equation was developed as an algorithmic subroutine and was integrated into current analysis software. The algorithm was then applied successfully to a full range of various test images. The PSF used was a Gaussian derived from the measured Full Width Half Maximum (FWHM) of an image of a star in the focal plane of the Whipple 10m telescope.

### 3. Observations and Analysis

To test the deconvolution process on real data, a group of 10 ON/OFF Crab Nebula pairs were chosen from the 2003/2004 observing season. The selection was based on the proximity to a PSF measurement, consistency of weather conditions and source elevation. The FWHM of the PSF depended on the telescope elevation and varied between  $0.12^\circ$  and  $0.14^\circ$ , corresponding to elevations of between  $60^\circ$  and  $80^\circ$  respectively. The normal analysis procedures [8] were carried out on the data (including software padding) up to the point of zeroing the non-image pixels. At this point any negative pixels were zeroed in order to avoid errors arising from a small negative denominator in (3).

Once all negative pixels have been eliminated from the image, the deconvolution algorithm was applied to each image and iterated a number of times. It was found the images converged after about 14 iterations. The initial impact of the algorithm was the extended length of time the analysis procedure took (up to 50-60 minutes per ON/OFF run on a 2 GHz Pentium machine). Once the 14 iterations were completed, normal picture/boundary thresholds were applied to the resulting image, *i.e.*, non-image pixels were zeroed. From this point on, the data were analysed as normal, and the standard supercuts method [8] of selecting gamma rays was applied. By

<sup>1</sup> where

$$a = (1, m - K + 1)_{max}; \quad b = (m, I)_{min};$$

$$c = (1, n - L + 1)_{max}; \quad d = (n, J)_{min};$$

$$e = i + K - 1; \quad f = j + L - 1;$$

$$i = \{1, I\}; \quad j = \{1, J\}; \quad r = \{0, 1, 2, \dots\}.$$

$K, L$  are dimensions of  $S_{k,l}$  and  $I, J$  are dimensions of  $W_{i,j}$

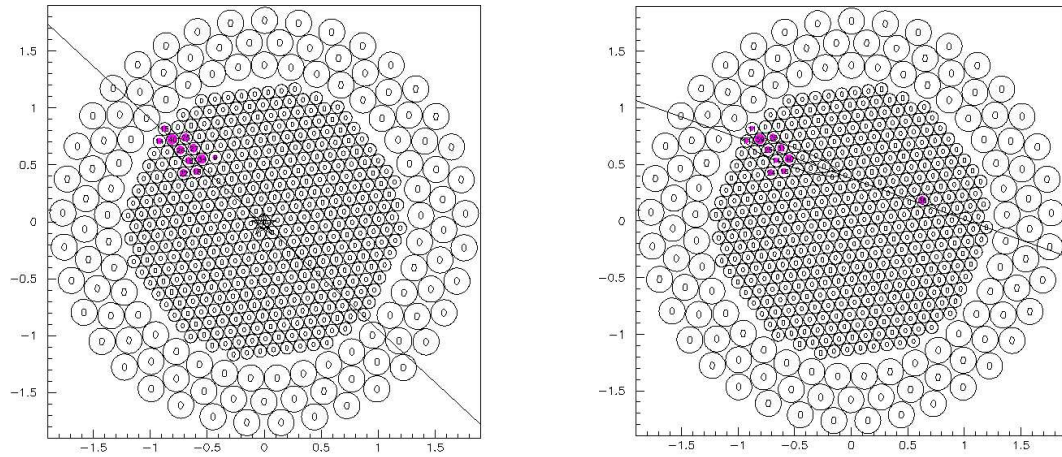


**Figure 1.** Candidate images before (left) & after deconvolution (right)

studying and comparing deconvolved and non-deconvolved images, it is clear that the deconvolution algorithm has by its nature increased the amount of light in the central region of the image. In other words, it has sharpened the image by gathering part of the image that was previously excluded from further analysis by the picture/boundary thresholds. The result of this effect is to increase the value of the size parameter of the image.

A further effect of the deconvolution was to increase the signal, in the same manner, in single or small groupings or islands of pixels in the camera, see Figure 1. When the signal in these island pixels is sufficient to pass the picture/boundary thresholds, they are included as image pixels and as such they cause a candidate  $\gamma$ -ray to be rejected later in the analysis when the parameter cuts are applied. This then necessitated a full re-optimisation of the picture/boundary threshold levels along with a re-optimisation of the parameter cuts. This was carried out using the test data mentioned above.

#### 4. Results

After an extensive analysis of the test data using a PSF value of  $0.14^\circ$ , the deconvolution did not lead to an increase in the significance of the analysis results. For each analysis a full re-optimisation of the picture/boundary levels and parameter cuts was carried out in order to find the maximum significance. The results of the optimisation in the form of a contour plot is shown in Figure 2. The figure shows contour levels of significance for various picture and boundary levels for un-deconvolved data (left) and deconvolved data (right). The resulting effect of the deconvolution is to shift the peak in significance to higher picture/boundary levels. However the peak value of the deconvolved data is not significantly increased compared to un-deconvolved data.

The peak signal seen from the data set before deconvolution was  $16.77\sigma$  with picture/boundary thresholds set at 3.00 and 5.00 respectively. After deconvolution a peak signal of  $16.99\sigma$  was found with picture/boundary thresholds set at 3.50 and 7.00. Looking at Figure 2 and comparing the two plots, it is clear that the deconvolution process is increasing the size parameter of the Cherenkov images, thus requiring higher picture/boundary threshold values to achieve a similar significance as that before deconvolution. It must be made clear that this increase in the size of the image is caused by the sharpening of the image. That is, part of the image signal that was previously omitted as it was not high enough to pass the picture/boundary thresholds is now being included to the final stages of the analysis.

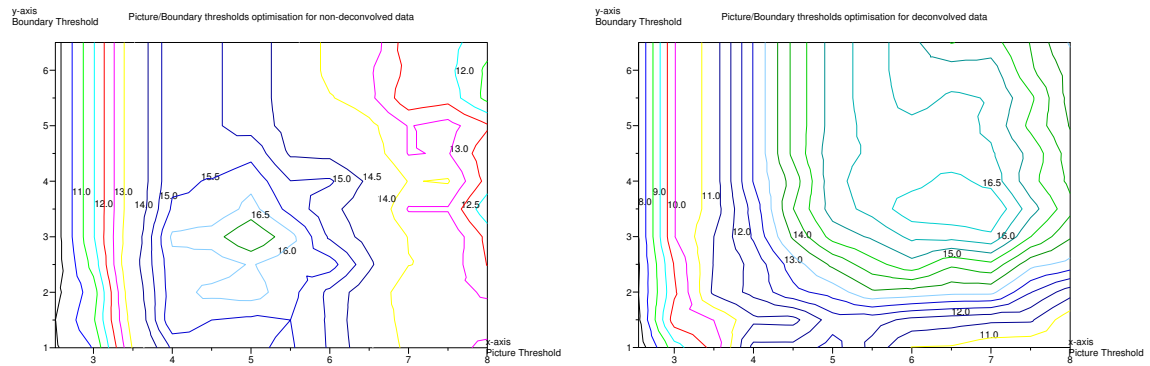


**Figure 2.** Contour plots of picture/boundary threshold optimisation before (Left) & after (right) deconvolution

We then applied the original and optimised cuts to an independent data set for comparison purposes. The standard cuts show a significance of  $10.13\sigma$ . After applying the optimised cuts to the un-deconvolved independent data set the significance dropped to  $8.71\sigma$ , and after deconvolution the significance was  $9.41\sigma$ .

## 5. Conclusions

We have demonstrated that the iterative deconvolution of the point spread function from Cherenkov images does not enhance the sensitivity of the atmospheric Cherenkov imaging technique.

## 6. Acknowledgements

The authors gratefully acknowledge the access given by the VERITAS Collaboration to its database of archived Crab Nebula data. This research project is supported by the Irish Research Council for Science, Engineering and Technology (IRCSET) Embark initiative funded by the National Development Plan and by Science Foundation Ireland.

## References

- [1] G. Ricort et al., *Pure Appl. Opt.*, 2, 125 (1993)
- [2] W.H. Richardson, *J. Opt. Soc. Am.* 62, 55 (1972).
- [3] L.B. Lucy, *Astron. J.* 79, 754 (1974).
- [4] J.L. Harris, Sr., *J. Opt. Soc. Am.* 56, 569 (1966).
- [5] B.L. McGlamery, *J. Opt. Soc. Am.* 57, 293 (1967).
- [6] *The international Dictionary of Mathematics* (Van Nostrand, N.J.), "Bayes' Theorem.", p.70 (1960).
- [7] R.E. Machol and P. Gray, *Recent Developments in information and Decision Process* (Macmillian, New York), p.175 (1962).
- [8] P.T. Reynolds et al., *Astrophys. J.* 404, 206 (1993).